



Published in final edited form as:

*Cancer Gene Ther.* 2011 October ; 18(10): 751–759. doi:10.1038/cgt.2011.51.

## Unreparable DNA Double Strand Breaks Initiate Cytotoxicity with HSV-TK/Ganciclovir

Brendon Ladd<sup>1,\*</sup>, Jessica J. O’Konek<sup>1,\*</sup>, Leo J. Ostruszka<sup>2</sup>, and Donna S. Shewach<sup>1</sup>

<sup>1</sup>Department of Pharmacology, University of Michigan Medical Center, Ann Arbor, MI 48109

<sup>2</sup>Accuri Cytometers, Ann Arbor, MI 48103

### Abstract

The herpes simplex virus thymidine kinase (HSV-TK) is the most widely used suicide gene in cancer gene therapy due to its superior anticancer activity with ganciclovir compared to other HSV-TK substrates, such as 1- $\beta$ -D-arabinofuranosyl thymine (araT). We have evaluated the role of DNA damage as a mechanism for the superiority of GCV. Using  $\gamma$ -H2AX foci as an indicator of DNA damage, GCV induced 7-fold more foci than araT at similarly cytotoxic concentrations. The number of foci decreased after removal of either drug, followed by an increase in Rad51 foci indicating that homologous recombination repair (HRR) was used to repair this damage. Notably, only GCV produced a late and persistent increase in  $\gamma$ -H2AX foci demonstrating the induction of unreparable DNA damage. Both drugs induced the ATR damage response pathway, as evidenced by Chk1 activation. However, GCV resulted in greater activation of ATM, which coincided with the late induction of  $\gamma$ -H2AX foci, demonstrating the presence of DNA double strand breaks (DSBs). The increase in DSBs after Rad51 induction suggested that they occurred as a result of a failed attempt at HRR. These data demonstrate that the late and unreparable DSBs observed uniquely with GCV account for its superior cytotoxicity and further suggest that inhibition of HRR will enhance cytotoxicity with HSV-TK/GCV.

### Keywords

gene therapy; ganciclovir; HSV-TK;  $\gamma$ -H2AX

### INTRODUCTION

While the initial goal of suicide gene therapy for cancer treatment was to maintain or increase tumor cell killing while sparing normal tissue toxicity, this approach also provided an opportunity to discover new drugs with potentially novel mechanisms of action that would lead to greater antitumor efficacy.<sup>1</sup> In addition, identifying the mechanism by which

Users may view, print, copy, download and text and data- mine the content in such documents, for the purposes of academic research, subject always to the full Conditions of use: [http://www.nature.com/authors/editorial\\_policies/license.html#terms](http://www.nature.com/authors/editorial_policies/license.html#terms)

Corresponding Author: Donna S. Shewach, Ph.D., 4742 Medical Sciences II, University of Michigan Medical Center, 1150 W. Medical Center Dr. Ann Arbor, MI 48109-5633, (734) 763-5810, (734) 763-3438 (fax), dshewach@umich.edu.

\*These authors contributed equally to this work

### Conflicts of interest:

The authors declare no conflicts of interest.

drugs used in suicide gene therapy elicit cytotoxicity may provide new, novel drug combinations that can enhance gene therapy without compromising its selectivity. One of the most widely used and studied suicide gene therapy approaches utilizes the herpes simplex virus thymidine kinase (HSV-TK) to activate the antiviral drug ganciclovir (GCV) to produce a non-traditional active metabolite with the potential for a novel mechanism of action leading to greater cancer cell killing. Indeed HSV-TK/GCV exhibits unique kinetics of cell killing and a remarkably mild effect on DNA synthesis that distinguishes it from traditional nucleoside analogs. The resulting excellent antitumor activity in preclinical studies has prompted numerous clinical trials, with promising results in a combination approach in patients with prostate cancer.<sup>2-4</sup>

HSV-TK/GCV is the most widely used suicide gene therapy approach both *in vitro* and *in vivo*. However, little attention has been focused on the mechanism by which it produces cell death. Similar to other nucleoside analogs, cytotoxicity requires activation of GCV (mediated by HSV-TK) to GCV 5'-triphosphate, which competes with dGTP for incorporation into DNA in internucleotide linkages.<sup>5,6</sup> While GCV shares this basic mechanism of cytotoxicity with other HSV-TK substrates, including the efficacious antivirals acyclovir (ACV) and 1- $\beta$ -D-arabinofuranosylthymine (araT), GCV induces multi-log cell killing at sub-micromolar concentrations, whereas ACV and araT were weakly cytotoxic at concentrations >100  $\mu$ M.<sup>5</sup> We have demonstrated previously that limited phosphorylation of ACV likely accounts for its poor cytotoxicity. However, araT is phosphorylated and incorporated to a greater degree than GCV, thus the reason for the inferiority of araT is not clear.

A few studies have attempted to address the mechanism by which GCV causes cell death. A study in B16 murine melanoma cells indicated GCV induced a morphological change in cells due to the reorganization of components of the cytoskeleton as well as an accumulation of cells in G2/M after a 48–72 hr incubation.<sup>7</sup> It has also been reported that GCV treatment results in a decline in Bcl-2 levels and activation of caspases, leading to apoptosis.<sup>8</sup> While these studies highlight pathways utilized by GCV that lead to cell death, they do not address the mechanism by which GCV is many logs more cytotoxic than other HSV-TK substrates. To begin addressing the consequences of GCV in DNA, Thust et. al demonstrated that GCV induced sister chromatid exchanges and chromosome breaks and translocations, whereas another substrate for HSV-TK, ACV, did not.<sup>9,10</sup> In light of the fact that sister chromatid exchanges arise as a consequence of homologous recombination repair (HRR),<sup>11</sup> these results suggest that DNA damage and pathways involved in its repair differ significantly between these drugs.

In a comparison of the events that lead to cytotoxicity for GCV and araT, we reported a unique manner of delayed cell death in response to GCV.<sup>5</sup> Cells completed one cell division after incubation with GCV. However, when they attempted to progress through the cell cycle for a second time, they were blocked in S phase where they remained until cell death occurred. In contrast, cells treated with araT accumulated in S phase and growth was inhibited for at least two days after drug washout, but subsequently cells progressed through the cell cycle and the cell number increased. This suggests that, with GCV treatment, an event occurring during this second round of DNA replication caused cells to permanently

arrest in S phase, resulting in cell death whereas araT produced greater disruption during the first S-phase.

In order to further understand the mechanisms by which these drugs elicited cytotoxicity, we evaluated the consequences of DNA incorporation for GCV and araT. We hypothesized that the distinct cell cycle kinetics of cell death with GCV and araT would result in measurable differences in the induction of a DNA damage response. Therefore, we wished to measure the extent and time course of DNA damage and its repair following treatment with GCV compared to araT. In addition, we evaluated a role for homologous recombination repair (HRR), as our previous studies in a yeast model indicated this repair pathway could rescue cells from GCV cytotoxicity,<sup>12</sup> and prior reports of sister chromatid exchanges promoted by GCV<sup>9,10</sup> suggested a role for HRR. Furthermore, we evaluated the extent to which each drug activated the two major DNA damage response pathways, mediated by ATR and ATM. Collectively, the results demonstrate a dramatic difference in the type and degree of DNA damage with GCV relative to araT, leading to distinct mechanisms of cell death.

## Materials and Methods

### Cell Culture

U251 human glioblastoma cells were maintained in exponential growth in RPMI 1640 medium supplemented with 10% calf serum (GIBCO, Grand Island, NY) and L-glutamine (Fisher Scientific, Pittsburgh, PA) in a humidified atmosphere at 37°C with 5% CO<sub>2</sub>. For stable expression of HSV-TK, U251 cells were transduced with a retroviral vector encoding the herpes simplex virus type 1 thymidine kinase, using the retrovirus long terminal repeat for a promoter, and the neomycin resistance gene for selection as previously described.<sup>5</sup> HSV-TK-expressing cells were selected with G418, and individual clones were expanded and maintained in medium containing G418. HSV-TK expression was determined by incubating cells with GCV and measuring phosphorylated GCV metabolites in cell lysates.

### Analysis of $\gamma$ -H2AX foci formation by laser scanning confocal microscopy

Cells were grown on chambered slides for 48 hr prior to drug addition. After incubation with drug, the cells were washed with PBS and then fixed and permeabilized with acetone/methanol (50:50 v/v) for 10 min. The fixed cells were then washed with PBS, blocked with 10% goat serum for 1 h, incubated with  $\gamma$ -H2AX primary antibody (1:400 dilution; Upstate, Charlottesville, VA) for 1 h, washed, incubated with AlexaFluor 488 conjugated goat anti-rabbit secondary antibody (1:200 dilution; Molecular Probes, Eugene, OR) for 1 h, washed and mounted with ProLong antifade kit (Molecular Probes, Eugene, OR). Slides were imaged with a Zeiss LSM510 confocal microscope using a 60 $\times$  objective lens. Images of representative cell populations were captured, and  $\gamma$ -H2AX foci were counted visually. At least 5 – 16 cells per well were counted with triplicate wells per condition, and each experiment was performed at least three times.

### Analysis of Rad51 foci formation by laser scanning confocal microscopy

Cells were grown on chambered slides for 48 hours prior to drug addition. Drug was added for 24 hours unless otherwise noted. At specified time points, cells were washed with PBS

and permeabilized with Triton-X buffer (0.5% Triton, 20mM Hepes, 50 mM NaCl, 3 mM KCl, 300mM Sucrose) for 5 min. Permeabilized cells were then fixed with paraformaldehyde solution (3% PFA, 2% sucrose, 1X PBS) for 30 min, washed 3 times for 10 minutes in wash buffer (0.5% NP40, 0.3% Sodium Azide, 1X PBS), blocked with 10% goat serum for 1 hour, and incubated with rabbit anti-Rad51 primary antibody (1:1600 dilution; Calbiochem, La Jolla, CA) for 1.5 hours. Cells were then washed 3 times in wash buffer, incubated with AlexaFluor 488 conjugated goat anti-rabbit secondary antibody (1:2000 dilution; Molecular Probes, Eugene, OR) for 1 hour, washed 3 times in wash buffer then washed with DAPI (.1µg/ml DAPI in 1X PBS) and mounted with ProLong antifade kit (Molecular Probes, Eugene, OR). Slides were imaged with an Olympus FV500 confocal microscope using a 100× objective lens. Images of representative cell populations were captured, and Rad51 positive cells were scored visually (cells with 10 foci were considered positive). At least 63 – 260 cells per well were scored with triplicate wells per condition, and each experiment was performed at least three times. Statistical significance was determined using a t-test.

#### **Analysis of $\gamma$ -H2AX and BrdUrd immunostaining by laser scanning confocal microscopy**

Cells were grown on chambered slides for 48 hr prior to drug addition. Cells were incubated with 30 µM BrdUrd for 30 minutes at the conclusion of drug incubation. Cells were fixed, permeabilized, and stained for  $\gamma$ -H2AX as described above, using AlexaFluor 594 conjugated goat anti-rabbit secondary antibody. After the final wash, antibody complexes were fixed with 3.7% paraformaldehyde in PBS for 10 minutes. Cells were treated with 2.5 N HCl for 30 minutes at 37°C and stained with AlexaFluor 488 mouse anti-BrdUrd conjugate (1:20 dilution, BD Pharmingen, San Jose, CA) for 1 hr. Slides were mounted and imaged as described above. At least 14 – 58 cells per well were counted with triplicate wells for each condition, and the experiment was performed at least twice. Percent positive cells were calculated as the number of cells positive for the indicated marker (BrdUrd or  $\gamma$ -H2AX) divided by the total number of cells examined. Percent  $\gamma$ -H2AX positive cells that were also positive for BrdUrd was calculated as the number of cells positive for both markers divided by the number of BrdUrd positive cells.

#### **Analysis of $\gamma$ -H2AX expression by flow cytometry**

After drug incubation, cells were harvested by trypsinization and washed with PBS. The pellets were resuspended in ice-cold PBS followed by the addition of cold 2% paraformaldehyde. Samples were then incubated at 4°C for a minimum of 30 min. Fixed samples were centrifuged and the pellets were resuspended in PBS containing 0.5% Tween 20 and incubated at 3°C for 15 min. PBS containing 0.5% Tween 20 and 5% serum (PBT) was added followed by centrifugation. Pellets were then resuspended in PBT. Anti- $\gamma$ -H2AX antibody was added to each sample and incubated for 45 min at room temperature and then washed with PBT. The pellets were then resuspended in anti-rabbit phycoerythrin conjugate antibody (Sigma Chemical Co, St. Louis, MO) and incubated for 45 min at room temperature. Samples were washed with PBT and resuspended in 7-Amino Actinomycin D (7-AAD) (Molecular Probes, Eugene OR) and incubated at room temperature for at least 30 min prior to flow cytometric analysis. Analysis was performed on BD FACS Calibur at the

University of Michigan Flow Cytometry Core Facility. At least 10,000 cells were evaluated for each condition, and the experiment was performed at least three times.

### Western Blot

All western blots for Chk1(Cell Signaling), pChk1(Ser317)(Cell Signaling), and actin (Calbiochem) were performed on 10% polyacrylamide gels according to standard protocols. Western blots for ATM (Epitomics) and pATM(Ser1982) (Epitomics) were performed as described above with exceptions: resolving gels were 6% polyacrylamide, transfer buffer contained 10% methanol and transfers were carried out at 300 mA overnight at 4°C. All secondary antibodies were HRP conjugated and from Santa Cruz. Phospho-ATM bands were quantitated using Image J software from the NIH, version 1.41.

## RESULTS

$\gamma$ -H2AX foci were used to identify sites of DNA damage, such as DNA double strand breaks (DSBs) or stalled replication forks.<sup>13–17</sup> Measurement of  $\gamma$ -H2AX foci demonstrated a dose-dependent increase in  $\gamma$ -H2AX foci after a 24 hr incubation with GCV in U251tk cells, relative to untreated control cells (Fig. 1A and B). Incubation with the non-cytotoxic IC<sub>10</sub> (0.03  $\mu$ M) for GCV resulted in a 4.4-fold increase ( $\pm 2.9$ ) in  $\gamma$ -H2AX foci which was not significantly different from control ( $p = 0.3$ ). Treatment with the IC<sub>50</sub> (0.05  $\mu$ M) or IC<sub>90</sub> (0.2  $\mu$ M) for GCV, however, significantly increased the number of  $\gamma$ -H2AX foci per cell ( $14.3 \pm 6.3$  fold and  $24.4 \pm 6.8$  fold, respectively;  $p < 0.001$ ) indicating a substantial increase in DNA damage.

$\gamma$ -H2AX expression was also assayed by flow cytometry in order to evaluate the effect of increasing drug concentrations on total  $\gamma$ -H2AX fluorescence. In untreated control cells, only 2% of the cells expressed detectable levels of  $\gamma$ -H2AX. Treatment with 0.2 and 1  $\mu$ M GCV (IC<sub>90</sub>) for 24 hr significantly increased the percentage of cells expressing  $\gamma$ -H2AX to 20% ( $p < 0.01$ ) and 59% ( $p < 0.001$ ), respectively (Figs 1C and D). Thus, two different independent methods have demonstrated an increase in  $\gamma$ -H2AX with increasing GCV concentration. Because quantifying the number of sites of DNA damage per cell provided a more definitive assessment of the extent of DNA damage compared to measuring simply the percentage of cells positive for  $\gamma$ -H2AX, subsequent experiments measured DNA damage using *in situ* immunohistochemistry.

Previously we have demonstrated that, although cell cycle progression is slowed during incubation with GCV, cells completed S-phase and divided. The lethal insult occurred during the second S-phase when cells were permanently arrested. Therefore we hypothesized that the DNA damage observed during GCV incubation (Fig. 1) was repaired enabling completion of the first S-phase, but additional DNA damage was incurred during the second S-phase. To test this hypothesis, U251tk cells were treated with either non-toxic (IC<sub>10</sub>) or cytotoxic (IC<sub>50</sub>, IC<sub>90</sub>) concentrations of GCV for 24 hr and assayed for  $\gamma$ -H2AX foci formation (Fig 3). At each concentration of GCV tested, an increase in foci was apparent within 12 hr after drug addition, continued through the end of the incubation, and decreased by 12 hr after drug washout. At the IC<sub>10</sub> for GCV, the number of foci was <5-fold greater than control levels throughout the 48 hr post-washout period. The two cytotoxic

concentrations of GCV produced a considerably greater number of  $\gamma$ -H2AX foci, increasing to ~15 – 25-fold higher than control at the conclusion of the incubation. This high level of DNA damage appeared to be repaired, as the number of  $\gamma$ -H2AX foci decreased to 5-fold more than control by 12 hr after drug washout without a substantial decrease in cell number. However, after 24 hr following washout of GCV at the IC<sub>50</sub> or IC<sub>90</sub>, the number of foci increased to greater than 10-fold over control, at which point massive loss of cells was apparent.

In view of the fact that cells treated with GCV arrest permanently during the second round of DNA replication following drug incubation,<sup>5</sup> we wished to verify that the presence of DNA damage at that time, indicated by  $\gamma$ -H2AX foci, predominated in S phase cells. Cells were treated with either no drug (control) or GCV (IC<sub>10</sub>, IC<sub>50</sub> and IC<sub>90</sub>) for 24 hr, then incubated with 5-bromo-2'-deoxyuridine (BrdUrd) for 30 min to identify cells actively replicating DNA, followed by staining for both BrdUrd in DNA and  $\gamma$ -H2AX. At drug washout (0 hr), the majority of  $\gamma$ -H2AX positive cells were in S phase, as indicated by BrdUrd incorporation, with a decrease to approximately one-quarter to one-half of  $\gamma$ -H2AX positive cells in S-phase by 24 hr after GCV washout (Table 1). At 48 hr after washout of GCV at its IC<sub>50</sub>, more than 70% of  $\gamma$ -H2AX labeled cells were in S-phase. Although cells treated with the IC<sub>90</sub> for GCV were not positive for BrdUrd at this time point, previously we have demonstrated that these cells are in S phase (propidium iodide staining) but with DNA synthesis decreased by more than 80%.<sup>5,18</sup> Thus, the large increases in  $\gamma$ -H2AX foci observed with cytotoxic concentrations of GCV occurred primarily in S-phase cells. In particular, cells dying in the second S-phase incurred significant DNA damage.

For comparison, we measured the effect of araT on  $\gamma$ -H2AX foci formation. After incubation of U251tk cells with the IC<sub>10</sub>, IC<sub>50</sub>, and IC<sub>80</sub> for araT (1  $\mu$ M, 11  $\mu$ M, and 100  $\mu$ M, respectively) for 24 hr, a concentration-dependent increase in  $\gamma$ -H2AX foci was observed (Fig 3A and B). However, the magnitude of foci formation was considerably less with araT (2 – 3.5-fold increase compared to control) relative to a similarly or less cytotoxic concentration of GCV (15 – 25-fold increase at IC<sub>50</sub> and IC<sub>90</sub>, respectively; Fig 1B).

Evaluation of the kinetics of foci formation with araT (IC<sub>50</sub>) during a 24 hr incubation revealed a small increase in the number of  $\gamma$ -H2AX foci (2.25-fold greater than control). The number of foci decreased by 12 hr after drug washout and remained slightly higher (approximately 1.7-fold) compared to control cells. No further increase was observed for up to 96 hr after washout (Fig. 3C). Thus both the degree and pattern of DNA damage was substantially different with araT relative to GCV. The number of foci in response to araT was not greater than that produced by the IC<sub>10</sub> (non-cytotoxic) for GCV, suggesting that the damage indicated by  $\gamma$ -H2AX foci was not sufficient to account for the cytotoxicity of araT.

The kinetics of  $\gamma$ -H2AX foci formation observed with cytotoxic concentrations of GCV suggested that the initial drug-induced DNA damage was repaired, consistent with our finding that the cells completed progression through the cell cycle,<sup>5</sup> but the secondary onset of damage was not repaired (Fig. 2). In contrast, damage initiated by araT appeared to be repaired prior to drug washout without further evidence of DNA damage thereafter. Because we have previously demonstrated that araT and GCV produce S-phase accumulation and a

slowing of DNA replication, we wished to determine whether HRR, the primary repair pathway for stalled replication forks and DNA DSBs during S-phase<sup>19,20</sup> was utilized to repair the damage. Following addition of GCV or araT, Rad51 positive cells were measured as an indicator of HRR.<sup>21</sup>(Fig. 4) For both drugs, the number of Rad51 foci increased after drug addition and through 12 hr post drug washout, after which foci decreased but remained elevated for at least another 60 hr. Analysis of the number of foci per cell in positive cells only revealed no significant difference between GCV and araT (data not shown). Thus, both drugs produced a similar activation of Rad51.

With evidence of DNA damage and its repair, we wished to determine the pathway responsible initiation of the  $\gamma$ -H2AX response. Thus, we evaluated the extent to which cells utilized the DNA damage response pathways initiated by ATR and/or ATM following GCV or araT exposure. In response to replication stress, ATR kinase is activated, and its activity can be measured by phosphorylation of its downstream target, Chk1 on serine 317. Western blot analysis revealed that Chk1 phosphorylation was most pronounced during incubation with araT, whereas it decreased rapidly following drug washout and persisted at low levels at all subsequent time points evaluated. These results are consistent with the strong DNA replication block that occurs during araT incubation but is relieved following drug washout.<sup>5</sup> GCV also induced an increase in Chk1 phosphorylation that was apparent both during and after drug incubation. These data indicate that, while both drugs initiated an ATR response, araT induced a more transient effect.

DNA damaging agents that produce DNA double strand breaks (DSBs) result in activation of ATM kinase, which can be detected by autophosphorylation at S1982. In response to araT (IC<sub>90</sub>), there was less than a 6-fold increase in ATM phosphorylation which persisted throughout the time course evaluated. When GCV (IC<sub>90</sub>) was added to cells, there was minimal activation of ATM during drug incubation. At 24 hr following drug washout, there was a dramatic increase in ATM phosphorylation, achieving an increase of nearly 20-fold by 72 hr post washout compared to control, indicating a strong DSB response. Together with the  $\gamma$ -H2AX data, ATM phosphorylation identifies the late-occurring DNA damage with GCV as DSBs, whereas cytotoxicity with araT is not due to a strong DSB response.

## DISCUSSION

Most nucleoside analogues elicit cytotoxicity through incorporation into DNA.<sup>22–24</sup> However, the extent and mechanism of cell killing can differ between these drugs even though their primary event leading to cytotoxicity is similar. We have demonstrated previously that GCV was more cytotoxic than araT, despite the fact that U251 cells incorporated at least 5-fold more araTMP than GCVMP into DNA, suggesting that the functional consequences of incorporation induced by these nucleoside analogues are different.<sup>5</sup> Here we have compared the extent and kinetics of DNA damage induced by exposure of tumor cells to GCV or araT, as well as the DNA damage response pathways utilized by these drugs. The results demonstrated that GCV induced significantly more DNA DSBs than araT at similarly cytotoxic concentrations as measured by  $\gamma$ -H2AX and ATM phosphorylation. The biphasic kinetics of DNA damage observed uniquely with GCV reflected the role of HRR in a failed attempt at DNA repair, leading to multi-log

cytotoxicity. Taken together, these data support a distinct mechanism for cell death with GCV compared to araT.

Previous studies have demonstrated that treatment of cells with ionizing radiation or cytotoxic drugs induces  $\gamma$ -H2AX foci formation in a dose-dependent fashion.<sup>17,25–27</sup> In the data presented here, we have used two different methods to demonstrate that induction of  $\gamma$ -H2AX increased in a dose-dependent manner with GCV. Following drug washout, the number of  $\gamma$ -H2AX foci decreased demonstrating that the cells were able to repair a portion of this damage. Time dependent resolution of foci formation has been demonstrated by others using ionizing radiation.<sup>15,25</sup> The results presented here differ in that we also observed an increase in  $\gamma$ -H2AX foci more than 24 hr after GCV washout, which to our knowledge has not been reported previously with other DNA damaging agents. This late increase in foci occurred only at the two cytotoxic concentrations of GCV (IC<sub>50</sub> and IC<sub>90</sub>), suggesting that this represents the lethal insult. Although the number of foci after GCV washout did not reach as high a level as observed during drug incubation, loss of cells due to cell death at this point interfered with our ability to quantify foci. Co-staining for  $\gamma$ -H2AX and BrdUrd demonstrated that most of the  $\gamma$ -H2AX foci were in S-phase cells, consistent with our previous data demonstrating an S-phase arrest at the times corresponding to the second increase in  $\gamma$ -H2AX foci. Association of the late increase in  $\gamma$ -H2AX foci at 48 hr after drug washout with cells in S-phase following induction of HRR suggests that the lethal insult occurred during attempted replication or repair of DNA. While many studies have focused on determining DNA damage during drug incubation, the studies presented here indicate that the critical events leading to cell death may occur long after drug washout.

Following exposure of cells to araT,  $\gamma$ -H2AX foci formation was strikingly different from that observed with GCV. While there was a dose-dependent increase in foci formation with araT, the maximum number of foci was at least 7-fold lower with araT despite the fact that more araTMP was incorporated into DNA.<sup>5</sup> This demonstrates that it is not simply the absolute amount of nucleotide analog incorporated into DNA but the consequences of that incorporation that is important for cytotoxicity. Furthermore, only GCV produced a second increase in  $\gamma$ -H2AX following drug washout that was coincident with cell death, demonstrating a role for late DNA damage in cytotoxicity. We have reported previously that apoptosis was induced similarly with both drugs, thus the increase in  $\gamma$ -H2AX foci following GCV treatment cannot be attributed to apoptosis.<sup>5</sup> These findings and the fact that the  $\gamma$ -H2AX produced by araT was similar to that observed with a non-cytotoxic concentration of GCV implicates a different mechanism of cell death for araT vs. GCV.

Previous reports demonstrate that GCV induces sister chromatid exchanges, suggesting a role for HRR in responding to GCV-induced DNA damage.<sup>9,10</sup> We investigated a role for HRR by analyzing Rad51 foci formation following treatment with GCV and araT. The results demonstrated that HRR was induced only after drug washout for both drugs. Because HRR responds to both stalled replication forks as well as DSBs, we further analyzed the DNA damage response pathways initiated by GCV and araT. The results demonstrated that both drugs activated ATR and ATM, though with strikingly different kinetics. The activation of ATR primarily during araT exposure indicated greater replicational stress induced by this drug, consistent with the greater inhibition of DNA synthesis by araT.<sup>5</sup> The



low activation of ATM during and after araT exposure suggests that this pathway was used to restart stalled replication forks. In contrast, GCV induced modest activation of ATR during and after drug exposure, consistent with its more moderate effect on DNA replication. GCV induced activation of ATM only after drug washout, as HRR declined. The concurrent increase in ATM activation and  $\gamma$ -H2AX foci after GCV indicates that the foci represent DSBs, consistent with reports by others of GCV-induced DSBs in other cell types.<sup>8</sup> A recent report also observed an increase in Chk1 phosphorylation, a late increase in activation of a downstream ATM substrate, Chk2, and an increase in  $\gamma$ -H2AX foci at a single late time point after addition of GCV and an adenovirus that transiently expressed HSV-TK.<sup>28</sup> However, these studies evaluated only a single, high concentration of GCV with variable amounts of adenovirus for transduction. Furthermore, they did not report controls for the effect of the adenovirus alone and thus the relative contribution of adenovirus transduction vs. GCV to the checkpoint alterations cannot be determined.

Based on our findings, we propose the following model for GCV cytotoxicity: During the first cell cycle, GCVMP incorporation into DNA slows DNA replication resulting in activation of ATR/Chk1 and a subsequent increase in  $\gamma$ -H2AX foci formation as the cell attempts to replicate past or correct this lesion. Completion of DNA replication, as evidenced by progression through the cell cycle, allows  $\gamma$ -H2AX foci to resolve. During the next entry into S-phase, GCVMP in the DNA template either doesn't serve as a good substrate for replication, or it is recognized as fraudulent and the cell attempts to repair it. DNA replication is halted and HRR is used in an attempt to restart replication and/or repair the lesion as evidenced by an increase in Rad51. However, GCVMP blocks HRR from successfully completing repair, and strong activation of ATM concurrent with  $\gamma$ -H2AX foci indicates formation of DSBs that prevent completion of S-phase resulting in massive cell death. In contrast, araT produced a strong activation of ATR during drug incubation and a modest increase in ATR and ATM activation in the absence of  $\gamma$ -H2AX foci after drug washout, consistent with successful restarting of stalled replication forks. These data indicate that araTMP in DNA can stall replication but the cell can successfully resume synthesis. In contrast, GCVMP is accommodated more readily in the nascent DNA, but it will not support replication when present in the DNA template.

In summary, the data demonstrate that the inability of HRR to repair GCV-mediated damage produced DSBs that resulted in cell death with GCV, whereas the mechanism of cell death with araT was distinctly different. Furthermore, at similarly cytotoxic concentrations DNA damage was less severe with araT and did not persist, whereas GCV induced greater DNA damage and it occurred in biphasic fashion. We suggest that GCVMP in the template blocked successful repair by HRR, leading to cell death. In contrast, we suggest that most of the DNA damage induced by araT was repaired, and cell effects other than direct DNA damage, such as signaling to cell death pathways,<sup>29</sup> results in cytotoxicity. These studies highlight that a novel mechanism accounts for the impressive antitumor activity of HSV-TK/GCV suicide gene therapy. These findings suggest that combining HSV-TK/GCV with approaches that compromise HRR will produce synergistic antitumor effects.

## Acknowledgments

This work was supported in part by grants CA076581 and CA083081 from the NIH. The project described was supported by grant number GM007767 from NIGMS. Its contents are solely the responsibility of the authors and do not necessarily represent the official views of NIGMS. The immunohistochemistry work was performed in the Microscopy and Image-analysis Laboratory (MIL) at the University of Michigan, Department of Cell & Developmental Biology with the assistance of Shelley Almburg.

## Abbreviations

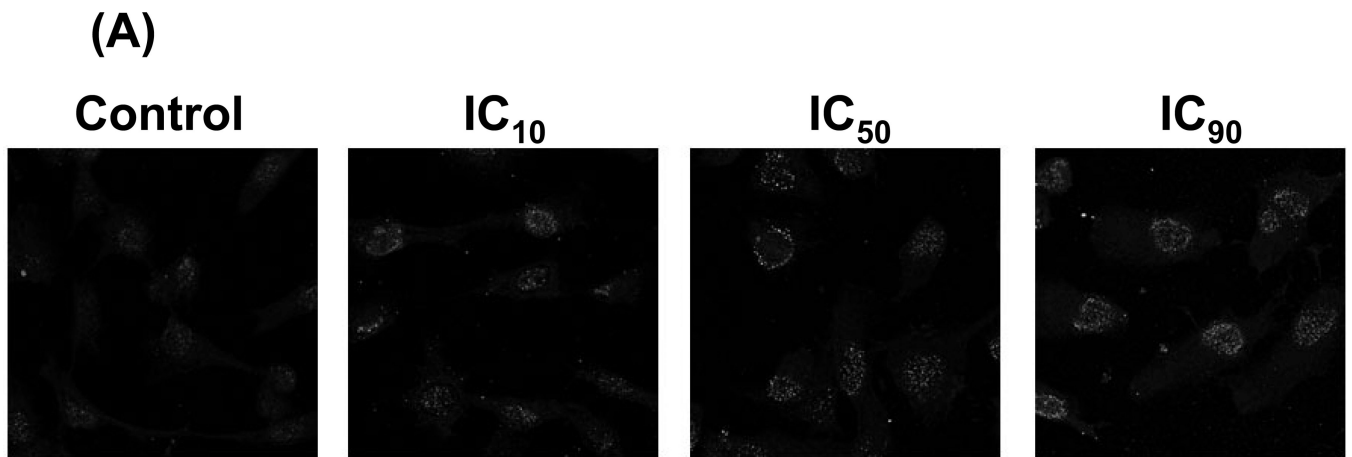
<b>GCV</b>	ganciclovir
<b>ACV</b>	acyclovir
<b>araT</b>	1- $\beta$ -D-arabinofuranosyl thymine
<b>araTMP</b>	araT monophosphate
<b>DSB</b>	double strand break
<b>GCVMP</b>	ganciclovir monophosphate
<b>GCVTP</b>	ganciclovir 5'-triphosphate
<b>HSV-TK</b>	herpes simplex virus thymidine kinase
<b>BrdUrd</b>	5'-bromo-2'-deoxyuridine
<b>HRR</b>	homologous recombination repair

## References

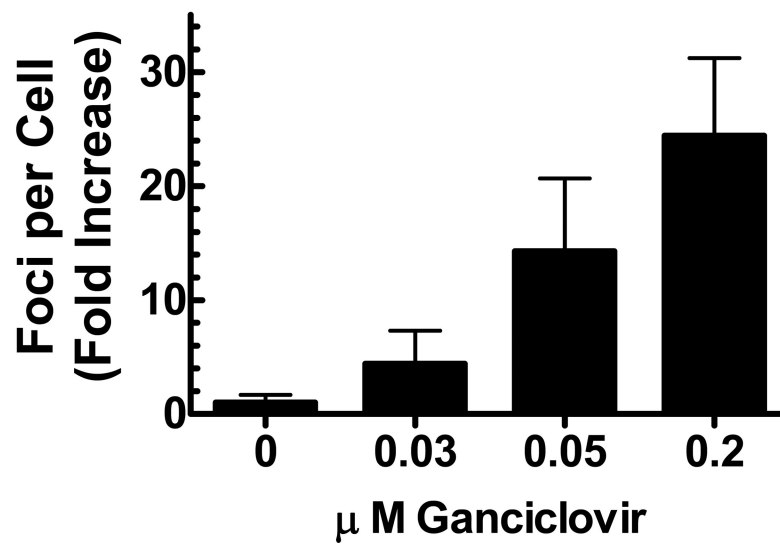
1. Moolten FL. Drug sensitivity ("suicide") genes for selective cancer chemotherapy. *Cancer Gene Ther.* 1994; 1:279–287. [PubMed: 7543006]
2. Roth JA, Cristiano RJ. Gene therapy for cancer: what have we done and where are we going? *J Natl Cancer Inst.* 1997; 89:21–39. [PubMed: 8978404]
3. Freytag SO, Khil M, Stricker H, Peabody J, Menon M, DePeralta-Venturina M, et al. Phase I study of replication-competent adenovirus-mediated double suicide gene therapy for the treatment of locally recurrent prostate cancer. *Cancer Res.* 2002; 62:4968–4976. [PubMed: 12208748]
4. Freytag SO, Stricker H, Pegg J, Paielli D, Pradhan DG, Peabody J, et al. Phase I Study of Replication-Competent Adenovirus-Mediated Double-Suicide Gene Therapy in Combination with Conventional-Dose Three-Dimensional Conformal Radiation Therapy for the Treatment of Newly Diagnosed, Intermediate- to High-Risk Prostate Cancer. *Cancer Res.* 2003; 63:7497–7506. [PubMed: 14612551]
5. Rubsam LZ, Davidson BL, Shewach DS. Superior Cytotoxicity with Ganciclovir Compared with Acyclovir and 1- $\beta$ -D-Arabinofuranosylthymine in Herpes Simplex Virus-Thymidine Kinase-expressing Cells: A Novel Paradigm for Cell Killing. *Cancer Res.* 1998; 58:3873–3882. [PubMed: 9731497]
6. Cheng YC, Grill SP, Dutschman GE, Nakayama K, Bastow KF. Metabolism of 9-(1,3-dihydroxy-2-propoxymethyl)guanine, a new anti-herpes virus compound, in herpes simplex virus-infected cells. *J Biol Chem.* 1983; 258:12460–12464. [PubMed: 6313660]
7. Halloran PJ, Fenton RG. Irreversible G2-M Arrest and Cytoskeletal Reorganization Induced by Cytotoxic Nucleoside Analogues. *Cancer Res.* 1998; 58:3855–3865. [PubMed: 9731495]
8. Tomicic MT, Thust R, Kaina B. Ganciclovir-induced apoptosis in HSV-1 thymidine kinase expressing cells: critical role of DNA breaks, Bcl-2 decline and caspase-9 activation. *Oncogene.* 2002; 21:2141–2153. [PubMed: 11948397]

9. Thust R, Tomicic M, Klocking R, Voutilainen N, Wutzler P, Kaina B. Comparison of the genotoxic and apoptosis-inducing properties of ganciclovir and penciclovir in Chinese hamster ovary cells transfected with the thymidine kinase gene of herpes simplex virus-1: implications for gene therapeutic approaches. *Cancer Gene Ther.* 2000; 7:107–117. [PubMed: 10678363]
10. Thust R, Tomicic M, Klocking R, Wutzler P, Kaina B. Cytogenetic genotoxicity of anti-herpes purine nucleoside analogues in CHO cells expressing the thymidine kinase gene of herpes simplex virus type 1: comparison of ganciclovir, penciclovir and aciclovir. *Mutagenesis.* 2000; 15:177–184. [PubMed: 10719044]
11. Sonoda E, Sasaki MS, Morrison C, Yamaguchi-Iwai Y, Takata M, Takeda S. Sister chromatid exchanges are mediated by homologous recombination in vertebrate cells. *Mol Cell Biol.* 1999; 19:5166–5169. [PubMed: 10373565]
12. O'Konek JJ, Boucher PD, Iacco AA, Wilson TE, Shewach DS. MLH1 deficiency enhances tumor cell sensitivity to ganciclovir. *Cancer Gene Ther.* 2009; 16:683–692. [PubMed: 19300472]
13. Rogakou EP, Pilch DR, Orr AH, Ivanova VS, Bonner WM. DNA double-stranded breaks induce histone H2AX phosphorylation on serine 139. *J Biol Chem.* 1998; 273:5858–5868. [PubMed: 9488723]
14. Sedelnikova OA, Rogakou EP, Panyutin IG, Bonner WM. Quantitative detection of (125)IdU-induced DNA double-strand breaks with gamma-H2AX antibody. *Radiat Res.* 2002; 158:486–492. [PubMed: 12236816]
15. Rogakou EP, Boon C, Redon C, Bonner WM. Megabase chromatin domains involved in DNA double-strand breaks in vivo. *J Cell Biol.* 1999; 146:905–916. [PubMed: 10477747]
16. Paull TT, Rogakou EP, Yamazaki V, Kirchgessner CU, Gellert M, Bonner WM. A critical role for histone H2AX in recruitment of repair factors to nuclear foci after DNA damage. *Curr Biol.* 2000; 10:886–895. [PubMed: 10959836]
17. Robinson BW, Ostruszka L, Im MM, Shewach DS. Promising combination therapies with gemcitabine. *Semin Oncol.* 2004; 31:2–12. [PubMed: 15199526]
18. O'Konek JJ, Ladd B, Flanagan SA, Im MM, Boucher PD, Thepsourinthone TS, et al. Alteration of the carbohydrate for deoxyguanosine analogs markedly changes DNA replication fidelity, cell cycle progression and cytotoxicity. *Mutation Research/Fundamental and Molecular Mechanisms of Mutagenesis.* 2010; 684:1–10. [PubMed: 20004674]
19. Rothkamm K, Kruger I, Thompson LH, Lohrich M. Pathways of DNA Double-Strand Break Repair during the Mammalian Cell Cycle. *Mol Cell Biol.* 2003; 23:5706–5715. [PubMed: 12897142]
20. Saleh-Gohari N, Helleday T. Conservative homologous recombination preferentially repairs DNA double-strand breaks in the S phase of the cell cycle in human cells. *Nucleic Acids Res.* 2004; 32:3683–3688. [PubMed: 15252152]
21. Wyman C, Ristic D, Kanaar R. Homologous recombination-mediated double-strand break repair. *DNA Repair (Amst).* 2004; 3:827–833. [PubMed: 15279767]
22. Plunkett W, Chubb S, Alexander L, Montgomery JA. Comparison of the toxicity and metabolism of 9-beta-D-arabinofuranosyl-2-fluoroadenine and 9-beta-D-arabinofuranosyladenine in human lymphoblastoid cells. *Cancer Res.* 1980; 40:2349–2355. [PubMed: 6966966]
23. Graham FL, Whitmore GF. Studies in mouse L-cells on the incorporation of 1-beta-D-arabinofuranosylcytosine into DNA and on inhibition of DNA polymerase by 1-beta-D-arabinofuranosylcytosine 5'-triphosphate. *Cancer Res.* 1970; 30:2636–2644. [PubMed: 5530558]
24. Parker WB, Shaddix SC, Chang CH, White EL, Rose LM, Brockman RW, et al. Effects of 2-chloro-9-(2-deoxy-2-fluoro-beta-D-arabinofuranosyl)adenine on K562 cellular metabolism and the inhibition of human ribonucleotide reductase and DNA polymerases by its 5'-triphosphate. *Cancer Res.* 1991; 51:2386–2394. [PubMed: 1707752]
25. Rothkamm K, Lohrich M. Evidence for a lack of DNA double-strand break repair in human cells exposed to very low x-ray doses. *Proc Natl Acad Sci U S A.* 2003; 100:5057–5062. [PubMed: 12679524]
26. Liu JS, Kuo SR, Melendy T. Comparison of checkpoint responses triggered by DNA polymerase inhibition versus DNA damaging agents. *Mutat Res.* 2003; 532:215–226. [PubMed: 14643438]

27. Ha L, Ceryak S, Patierno SR. Generation of S phase-dependent DNA double-strand breaks by Cr(VI) exposure: involvement of ATM in Cr(VI) induction of gamma-H2AX. *Carcinogenesis*. 2004; 25:2265–2274. [PubMed: 15284180]
28. Abate-Daga D, Garcia-Rodríguez L, Sumoy L, Fillat C. Cell cycle control pathways act as conditioning factors for TK/GCV sensitivity in pancreatic cancer cells. *Biochimica et Biophysica Acta (BBA) - Molecular Cell Research*. 2010; 1803:1175–1185. [PubMed: 20599444]
29. Tomicic MT, Bey E, Wutzler P, Thust R, Kaina B. Comparative analysis of DNA breakage, chromosomal aberrations and apoptosis induced by the anti-herpes purine nucleoside analogues aciclovir, ganciclovir and penciclovir. *Mutat Res*. 2002; 505:1–11. [PubMed: 12175901]



**(B)**



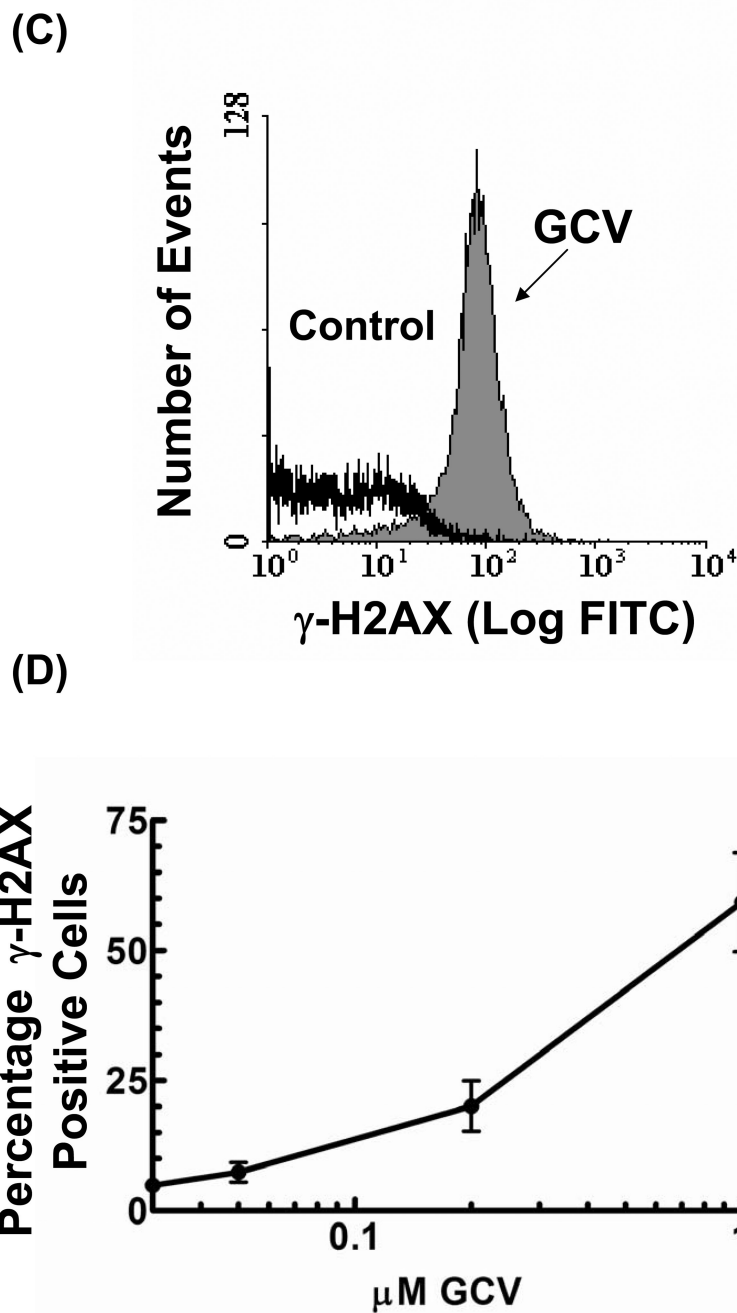


**Figure 1. GCV induces a dose-dependent increase in  $\gamma$ -H2AX**

U251tk cells were incubated with GCV for 24 hr and assayed for  $\gamma$ -H2AX foci formation.

(A) representative cells as captured by confocal microscopy; (B) quantitation of the number  $\gamma$ -H2AX foci per cell; (C) measurement of  $\gamma$ -H2AX expression by flow cytometry after a 24 hr incubation with 1 $\mu$ M GCV; (D) quantitation of percentage of  $\gamma$ -H2AX expressing cells from flow cytometry. Points represent mean of triplicate experiments; bars represent standard error.

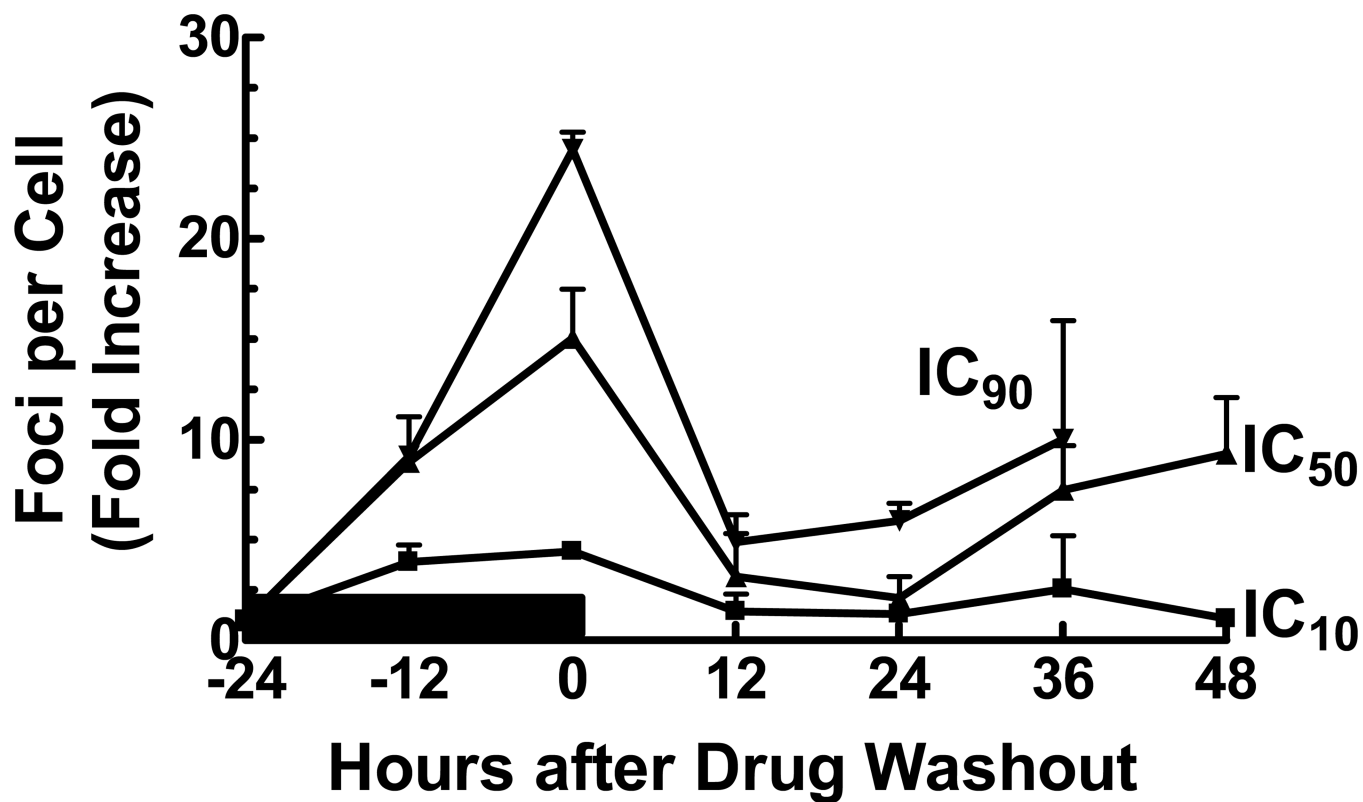
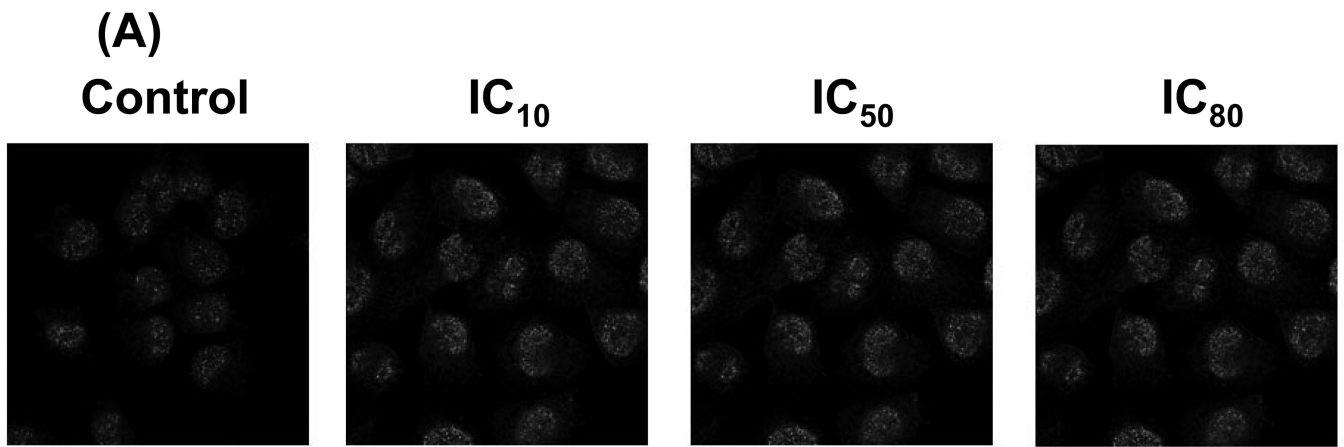
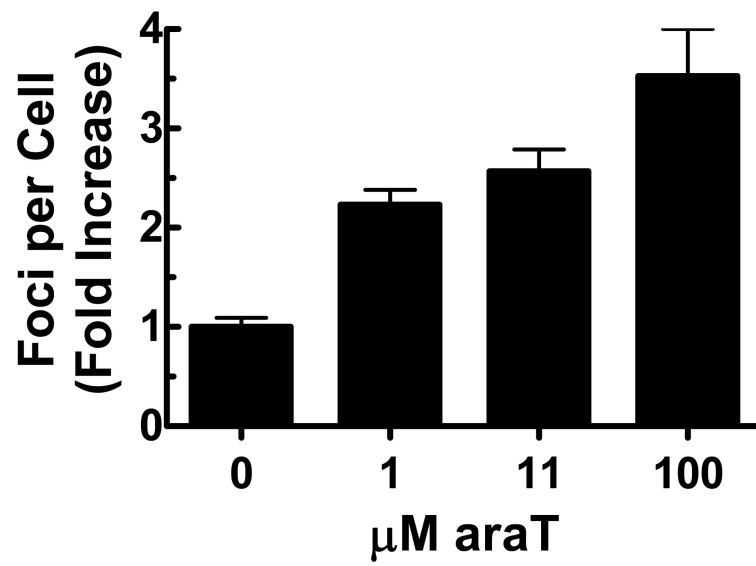


**Figure 2. Time course of  $\gamma$ -H2AX foci formation in response to GCV**  
U251tk cells were incubated with GCV at the IC<sub>10</sub>, IC<sub>50</sub> or IC<sub>90</sub> for 24 h followed by drug washout. Cells were assayed by confocal microscopy for  $\gamma$ -H2AX foci formation at the indicated time points. Black bar indicates duration of drug incubation, points represent the mean of at least three experiments, bars represent standard error.

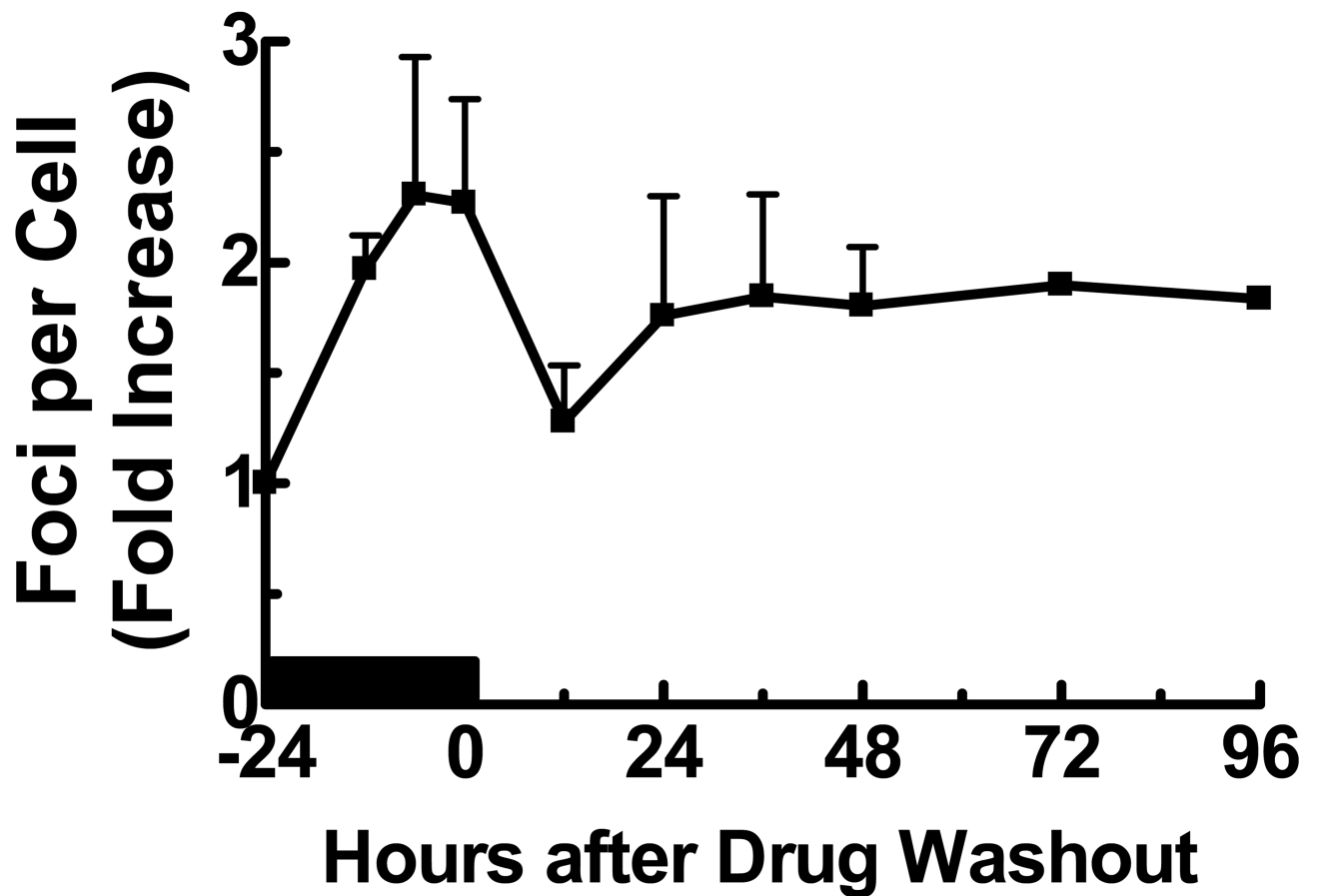


**(B)**





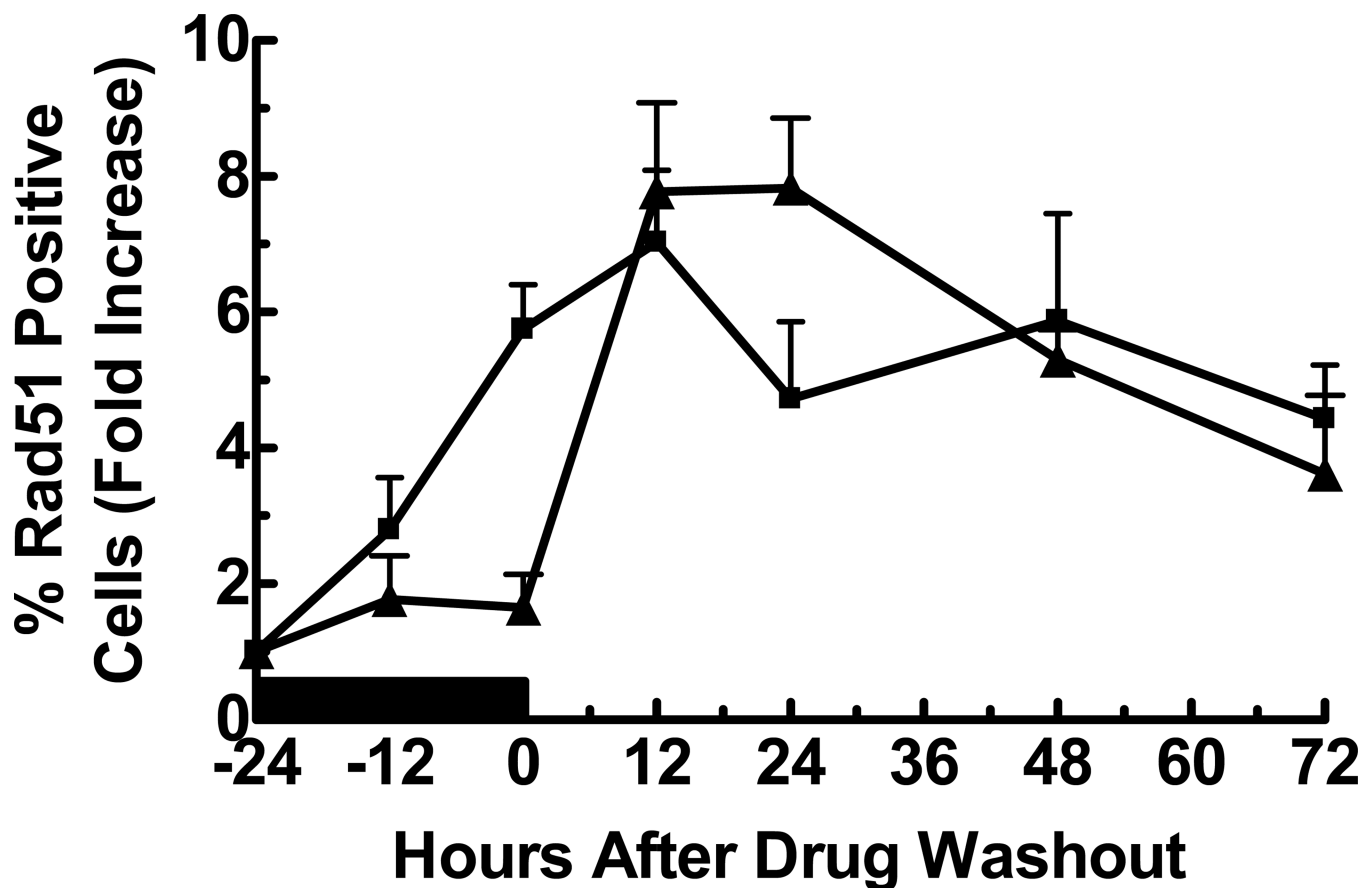
(C)



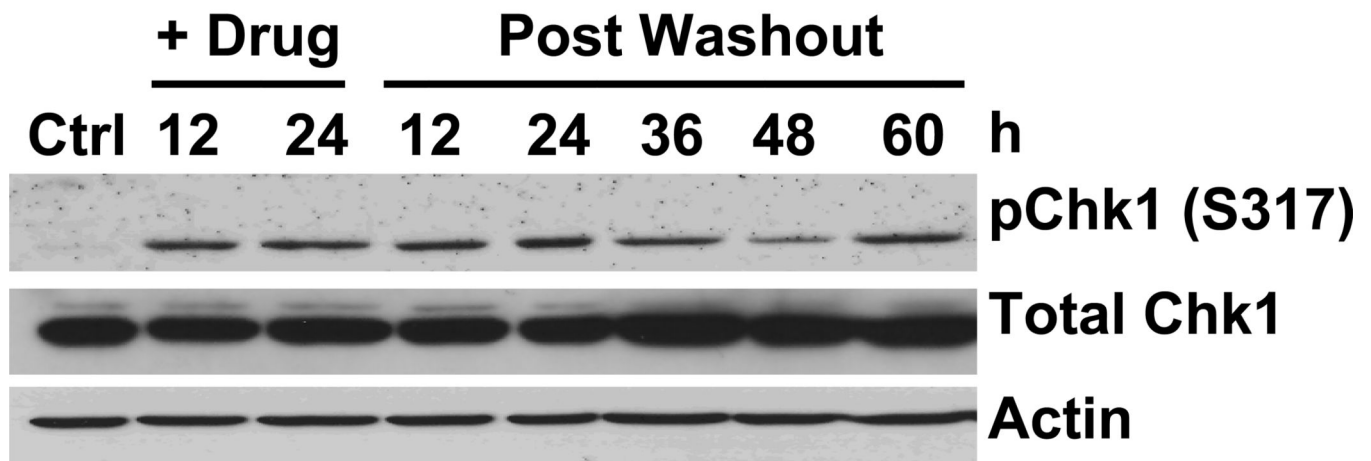
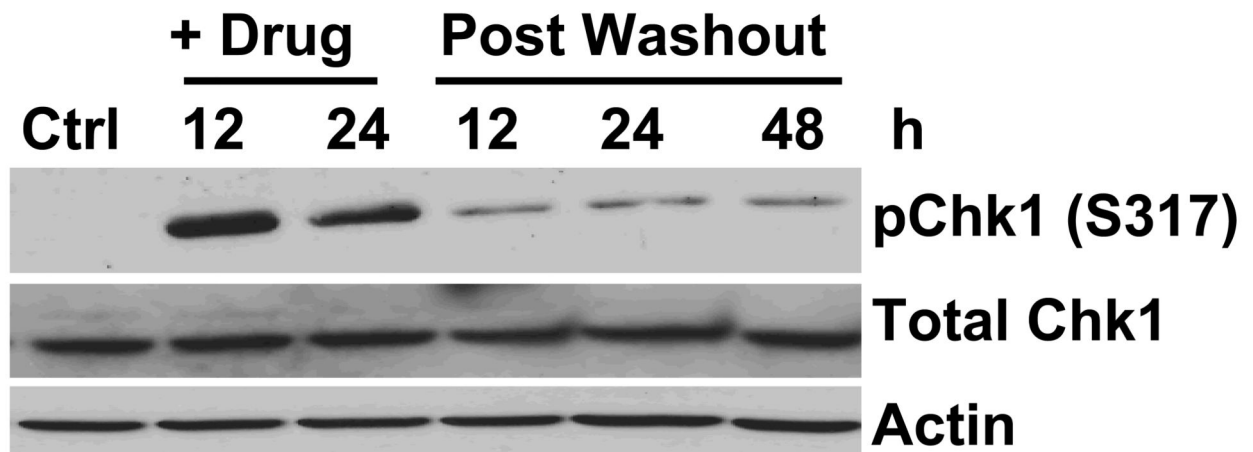
**Figure 3. araT induces a dose-dependent increase in  $\gamma$ -H2AX**

U251tk cells were incubated with araT for 24 hr and assayed for  $\gamma$ -H2AX foci formation.

(A) Representative cells as captured by confocal microscopy. (B) quantitation of the number  $\gamma$ -H2AX foci per cell. (C) U251tk cells were incubated with 100 $\mu$ M araT ( $IC_{80}$ ) for 24 hr followed by drug washout. Cells were assayed for  $\gamma$ -H2AX foci formation by confocal microscopy at the indicated time points and the number of  $\gamma$ -H2AX foci per cell was determined. Black bar indicates duration of drug incubation. Points represent the mean of at least three experiments, bars represent standard error.



**Figure 4. Time course of Rad51 foci formation in response to GCV or araT**  
U251tk cells were incubated with (▲) IC<sub>90</sub> GCV or (■) IC<sub>80</sub> araT for 24 h followed by drug washout. Cells were assayed by confocal microscopy for Rad51 at the indicated time points (positive cell = 10 Rad51 foci). Black bar indicates duration of drug incubation, points represent the mean of at least three wells from a representative experiment, bars represent standard error.

**(A) GCV****(B) araT**

**Figure 5. Time course of Chk1 phosphorylation in response to GCV or araT**  
 U251tk cells were incubated with (A) IC<sub>90</sub> GCV or (B) IC<sub>90</sub> araT for 24h followed by drug washout. pChk1(Ser317) was assayed by western blot at the indicated time points. Total Chk1 and actin were used as loading controls.

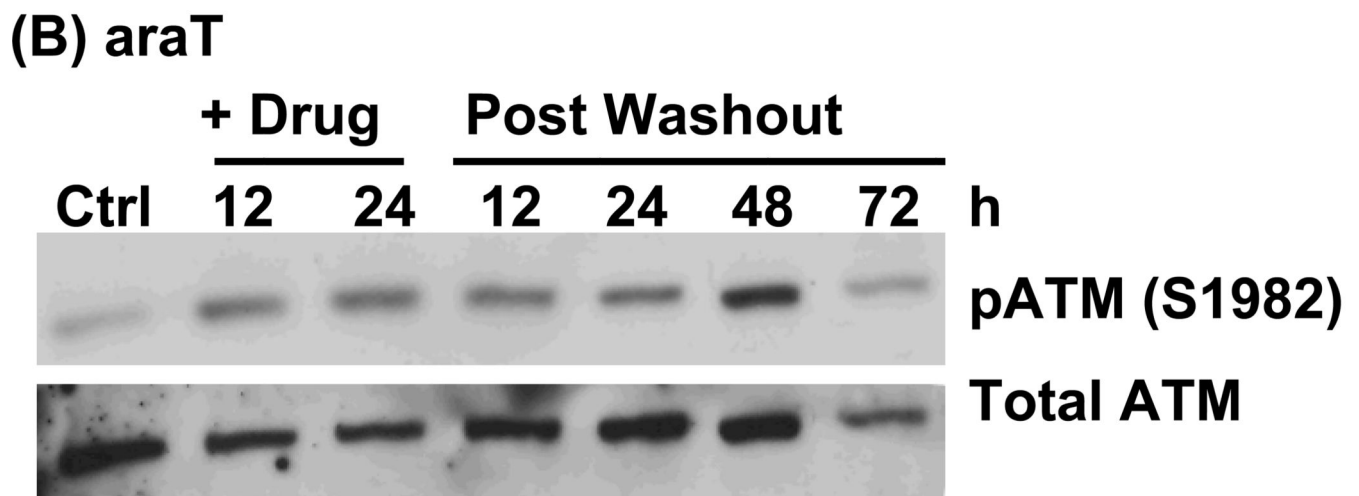
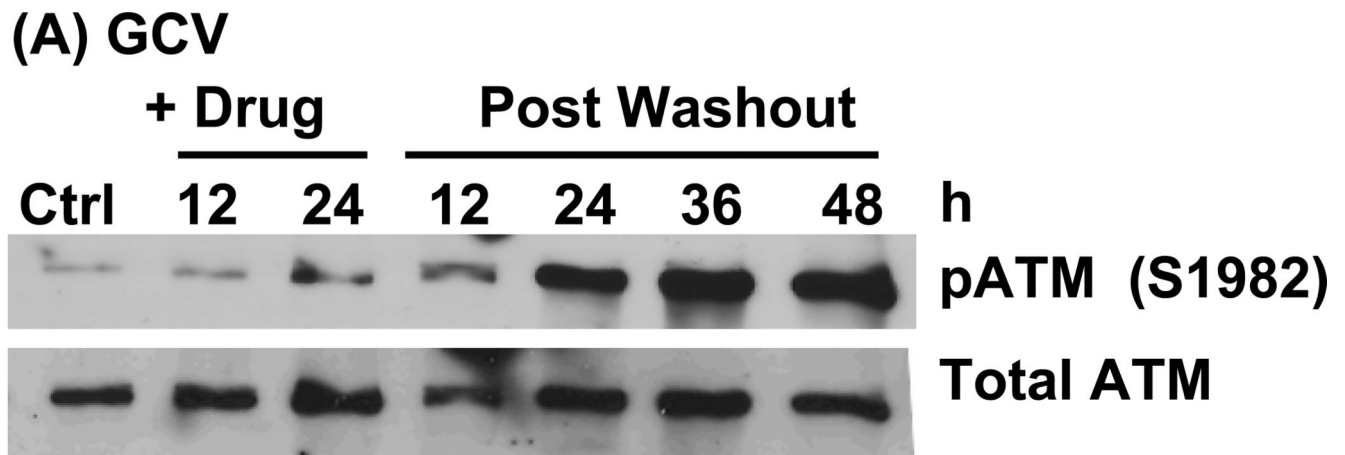


**Figure 6. Time course of ATM activation in response to GCV or araT**  
 U251tk cells were incubated with (A) IC<sub>90</sub> GCV or (B) IC<sub>90</sub> araT for 24h followed by drug washout. pATM (Ser1982) was assayed by western blot at the indicated time points. Total ATM was used as a loading control.

**Table 1**  
**Colocalization of  $\gamma$ -H2AX and BrdUrd in response to GCV**

U251tk cells were incubated with GCV at the indicated concentrations ( $IC_{10} = 0.03 \mu\text{M}$ ,  $IC_{50} = 0.05 \mu\text{M}$ ,  $IC_{90} = 0.2 \mu\text{M}$ ) for 24 h followed by drug washout. Cells were assayed for  $\gamma$ -H2AX foci formation and bromodeoxyuridine (BrdUrd) staining at the indicated time points. Time = 0 represents the time of drug washout. Values represent the percentage of cells that stained positive for  $\gamma$ -H2AX (contained greater than 5 foci), BrdUrd, or both. At least 50 cells were counted at each time point. n.d.= not determined.

		% BrdUrd Positive	% $\gamma$ -H2AX Positive	% of $\gamma$ -H2AX Positive that are also BrdUrd Positive
0 hr	C	46 $\pm$ 9	26 $\pm$ 16	67 $\pm$ 31
	$IC_{10}$	57 $\pm$ 6	59 $\pm$ 20	64 $\pm$ 17
	$IC_{50}$	65 $\pm$ 6	80 $\pm$ 16	79 $\pm$ 12
	$IC_{90}$	85 $\pm$ 21	95 $\pm$ 3	86 $\pm$ 19
24 hr	C	38	15	75
	$IC_{10}$	77 $\pm$ 28	11 $\pm$ 4	25 $\pm$ 35
	$IC_{50}$	63 $\pm$ 5	20 $\pm$ 3	41 $\pm$ 8
	$IC_{90}$	56 $\pm$ 62	72 $\pm$ 22	57 $\pm$ 61
48 hr	C	n.d.	n.d.	n.d.
	$IC_{10}$	38 $\pm$ 3	8 $\pm$ 5	70 $\pm$ 42
	$IC_{50}$	62 $\pm$ 8	72 $\pm$ 21	79 $\pm$ 14
	$IC_{90}$	0	90	0